A Single-Layer Ultra-Wideband Dual-Channel Differential Phase Shifter Using Coupled Lines

R. Kazemi*(C.A.), Z. Assadollahzadeh Zia*, and R. Masoumi*

Abstract: In this work, a broadband dual-channel differential phase shifter is developed with a small phase deviation across a wide frequency range. The design consists of two main lines for 45° and 90° phase shifts, along with a reference line. A prototype is fabricated and measured to validate the performance of the design. Phase shifts of $45° \pm 5°$ and $90° \pm 5°$ over a frequency range of 1.26 GHz - 4 GHz (bandwidth of 104%) are achieved from the channels. The transmission losses of the three lines are less than 0.35 dB and the isolation between the adjacent ports is better than 20 dB. The area of this dual-channel differential phase shifter is $0.22\lambda_g^2$ (14.7 mm × 66.15 mm), where λ_g is the guided wavelength at the center frequency.

1 Introduction

IN modern communication systems, to improve the radiation characteristics of an antenna in a particular direction, its input signal must be controlled. For this purpose, phase shifters apply specific amounts of time delay (or phase shift) to the transmitted signal. Phase shifters are one of the most important components of microwave systems. In modern communication and radar systems where security and multi-function capability are necessary, wideband phase shifters are required. Phase shifters can be classified into two major types, according to how to control the amount of phase shift: mechanical and electronic, which the second type is more common in phased array antennas [1].

Due to the growing need for efficient and wideband integrated systems, integrated phase shifters are required with minimal attenuation and phase deviation over a broad bandwidth. Coupled-line structures are suitable choices for broadband applications due to their low phase error and compact dimension [2]. Also, among

integrated phase shifters, microstrip differential phase shifters are extensively used in modern communication systems such as single-pulse radars, butler matrices, microwave measuring devices, modulators, and many other industrial applications [2]-[8].

In recent years, new phase shifters based on microstrip structures have been used due to their planar and compact dimension, wide bandwidth, low loss, simplicity, low manufacturing cost, and easy integration with planar circuits. To enhance the quality of the system, new techniques such as photonic band gap (PBG) [9], ground plane aperture (GPA) [10], defected ground structure (DGS) [11], etc. have been utilized. Broadband differential phase shifters are mainly based on Schiffman's design [4]. They consist of two lines; one is a reference microstrip line and the other line comprises two tightly coupled strips connected at the end. By accurately choosing the length and coupling of these lines, a relatively constant phase difference between two lines can be achieved over a wide frequency range.

In [12], a 45° differential microstrip phase shifter is designed for beam shaping networks; ±2.5° and ±5° phase errors are achieved with 51.8% and 64% bandwidths, respectively. It has a relatively low bandwidth despite having low transmission loss and compact dimensions. A 90° differential phase shifter using a weak coupled line is proposed in [13]; it is wideband and compact, but only offers a 90° phase shift.

In [14], a method is proposed to design a wideband phase shifter using microstrip lines and liquid crystal (LC), but it has a relatively high transmission loss of 2.5 dB in the frequency range of 220 GHz - 330 GHz. Two-phase shifters using substrate-integrated waveguide (SIW) and half-mode SIW (HMSIW) structures are studied in [15] and [16]. In [15], a new electronically controllable SIW phase shifter is introduced; in this design, two and four metal rods are utilized in the SIW transmission line for inductive and capacitive loading, respectively. Phase shift is generated by the metal rods. The proposed phase shifter operates over a wide bandwidth of 26 GHz - 32 GHz with a maximum simulated transmission loss of 3 dB and a phase shift of $100° ± 5°$. In [16], a compact and broadband phase shifter is designed using HMSIWs. The proposed phase shifter has phase shifts of $86° ± 2.5°$ and $43.5° ± 2.5°$ at center frequencies of 7.5 GHz and 8.4 GHz, which respectively have 53.3% and 35.7% bandwidths. The maximum transmission loss of this structure is 1.2 dB, which is relatively low and its dimensions are small. However, insufficient bandwidth is the main problem of this design and almost all SIW-based structures due to their cut-off frequencies. When compact circuits are required, phase shifters with filtered switches are used [17], [18]. This type of phase shifter occupies less chip area than other structures and has low transmission loss, although bandwidth is usually narrow.

In this paper, a wideband dual-channel phase shifter is proposed using coupled microstrip lines. It offers phase shifts of 45° and 90° over the bandwidth of 1.26 GHz – 4 GHz (104 %), i.e., the frequency range that is allocated for most commercial, satellite and personal communication bands such as Global Positioning System (GPS, 1.575 GHz), Personal Communications Service (PCS, 1.85 GHz – 1.99 GHz), WiBro (2.3 GHz – 2.39 GHz), Digital Communication Systems (DCS, 1.710 GHz – 1.880 GHz), WiMax (2.3 GHz – 3.7 GHz), Bluetooth (2.4 GHz), etc.

This paper is structured as follows. In section 2, the theory and design procedure of the dual-channel differential phase shifter are discussed. In section 3, the measured results of the fabricated prototype are compared with the simulation and analyzed. Section 4 gives the conclusion.

2 Theory and Design Procedure of the Dual-Channel Phase Shifter

The proposed dual-channel differential phase shifter is a six-port network consisting of two main lines along with a reference line designed to generate 45° and 90° phase shifts. The configuration of the proposed phase shifter is shown in Fig. 1. In this design, the first line is a coupled microstrip line connected to a short-circuited stub (90° channel, line 1); the second line is the common reference line and it is a simple microstrip line (line 0), and the third line is a short-end coupled line (45° channel, line 2).

2.1 Theoretical Analysis

The required phase shift is obtained from the phase difference between the signals passing through each of the main lines and the common reference line. Since the structure of the proposed phase shifter is symmetric, the even-odd mode technique along the vertical plane is used for analysis. The S-parameters of each line can be calculated through the equivalent circuit of even and odd modes. Even- and odd-mode decompositions of three lines are shown in Fig. 2.

At frequency f, the corresponding phase shifts (90°, 45°) between the main lines and the reference line are obtained from Eq. (1):

$$\Delta\Phi_1(f) = \angle S_{12}(f) - \angle S_{43}(f)$$
$$\Delta\Phi_2(f) = \angle S_{65}(f) - \angle S_{43}(f) \tag{1}$$

In the 90° main line, a short-circuited stub with a characteristic impedance of Z_s is connected to the end of

(a)   (b)   (c)
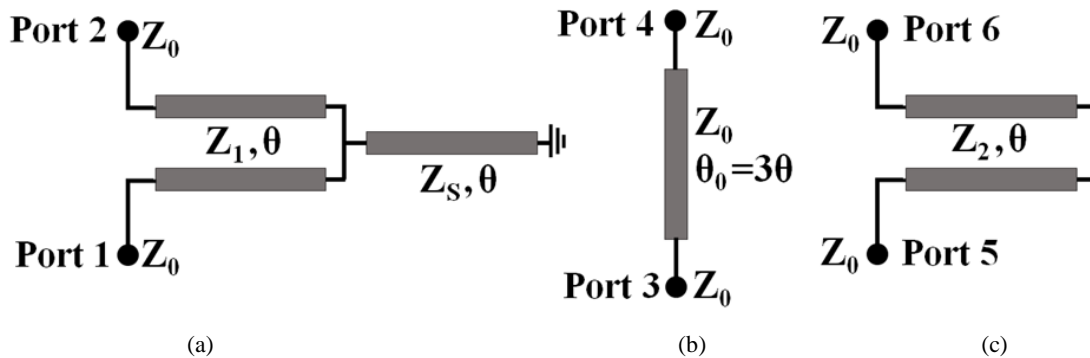
Fig. 1 The schematic of the proposed dual-channel differential phase shifter; (a) 90° main line (line 1), (b) reference line (line 0), (c) 45° main line (line 2).
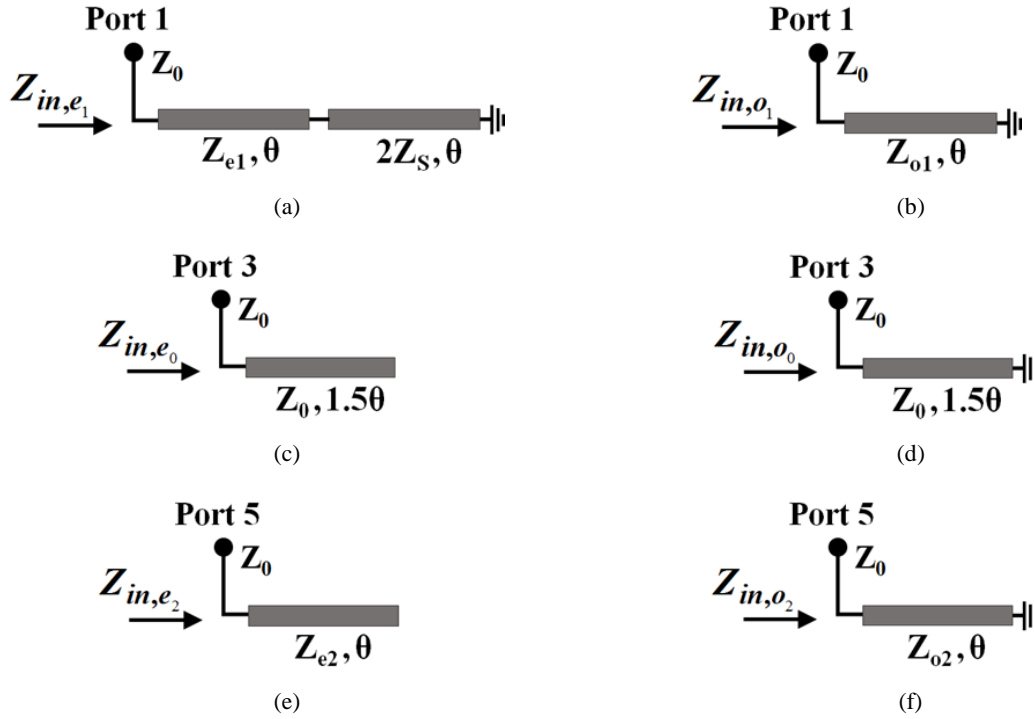
Fig. 2 The even-odd mode sub-circuits of the lines; (a) even mode and (b) odd mode of the 90° main line (line 1), (c) even mode and (d) odd mode of the reference line (line 0), (e) even mode and (f) odd mode of the 45° main line (line 2).

a coupled line with characteristic impedances of Z_{e1} and Z_{o1} for its even- and odd-modes, respectively. The short stub provides an extra degree of freedom. The common reference line is a simple microstrip transmission line with a characteristic impedance of Z_0 and an electrical length of $\theta_0 = 3\theta$; it is bent to occupy less space. The 45° main line is a short-end coupled line with characteristic impedances of Z_{e2} and Z_{o2} for its even and odd modes, respectively. The even- and odd-mode impedances, $Z_{in,e}$ and $Z_{in,o}$, for each line can be obtained as:

$$Z_{in,e_1} = jZ_{e1} \tan\theta \frac{2Z_s + Z_{e1}}{Z_{e1} - 2Z_s \tan^2\theta} \tag{2-a}$$

$$Z_{in,o_1} = jZ_{o1} \tan\theta$$

$$Z_{in,e_0} = -jZ_0 \cot(1.5\theta)$$
$$Z_{in,o_0} = jZ_0 \tan(1.5\theta) \tag{2-b}$$

$$Z_{in,e_2} = -jZ_{e2} \cot\theta$$
$$Z_{in,o_2} = jZ_{o2} \tan\theta \tag{2-c}$$

The transmission coefficient of the lines can be expressed as

$$S_{21,i} = \frac{1}{2} \left[\frac{Z_{in,e_i} - Z_0}{Z_{in,e_i} + Z_0} - \frac{Z_{in,o_i} - Z_0}{Z_{in,o_i} + Z_0} \right] \quad , \quad (i = 0,1,2) \tag{3}$$

and the phase shift of the lines can be further obtained as

$$\angle S_{21,i} = \tan^{-1} \left[\frac{Z_0^2 - Z_{in,e_i} \cdot Z_{in,o_i}}{Z_0(Z_{in,e_i} + Z_{in,o_i})} \right] \quad , \quad (i = 0,1,2) \tag{4}$$

According to the phase shift of the lines given in Eq. (4), the differential phase shifts are mainly determined by the electrical lengths and characteristic impedances of the lines. For simplicity of analysis, let the initial value of $\theta = 90°$ at the center frequency of $f_0 = 2.5$ GHz. Thus, the phase shifts are determined by the characteristic impedances of the lines ($Z_{e1}, Z_{o1}, Z_{e2}, Z_{o2}, Z_s$). By optimizing these parameters on the CST Microwave Studio software, we obtain the required phase shifts over the desired bandwidth.

2.2 3D Simulation

The proposed phase shifter is designed on a single-layer RO4003C substrate with a thickness of 0.813 mm, $\varepsilon_r = 3.38$, and $\tan\delta = 0.0027$. It is compatible with most integrated communication systems. The 3D structure of the dual-channel phase shifter simulated in CST Microwave Studio software is shown in Fig. 3. Its total size is 66.15
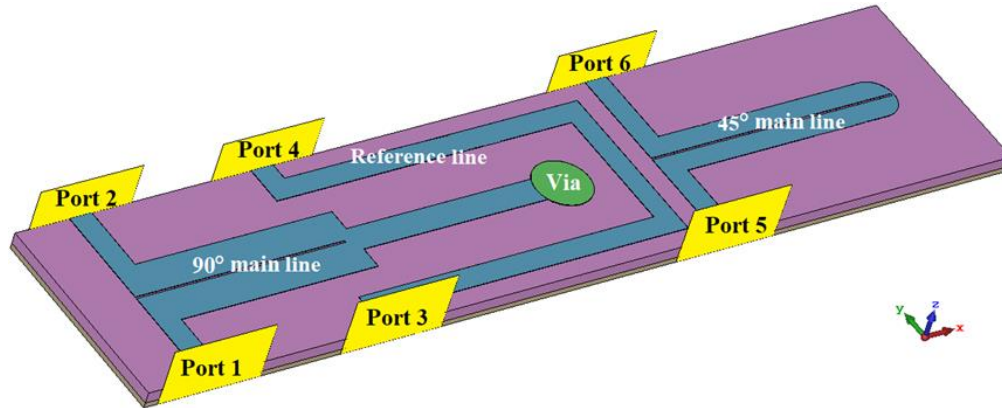
Fig. 3 3D layout of the dual-channel phase shifter simulated in CST Microwave Studio.
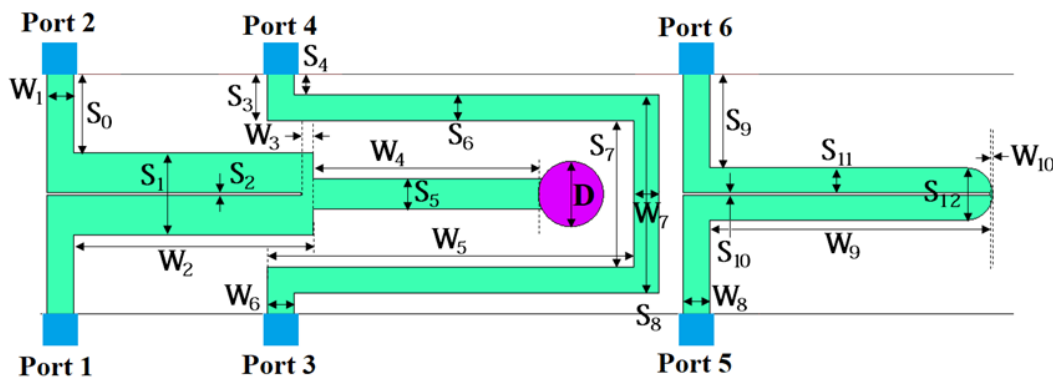

Fig. 4 The dimensional parameters of the proposed dual-channel phase shifter.

mm×14.7 mm ($1.01\lambda_g \times 0.22\lambda_g$). Fig. 4 shows the layout of the circuit with its optimized dimensions summarized in Table 1.

2.3 Parametric Study

A parametric analysis is carried out to investigate the effects of the short via in line 1 and the curved edge of line 3 on the phase shifter performance. First, the impact of the via size on the performance of the phase shifter is evaluated. Since it is located on the 90° main line, its impact on this channel's performance is critical. Thus, for brevity, the S-parameters of other ports are not shown.

According to Fig. 4, for the 90° main line, it is clear

Table 1 The optimized dimensions of the dual-channel phase shifter (in mm).

|							
W_1	1.66	W_7	1.55	S_2	0.15	S_8	12.12
W_2	14.73	W_8	1.66	S_3	2.87	S_9	5.75
W_3	0.75	W_9	17.21	S_4	1.29	S_{10}	0.15
W_4	13.83	W_{10}	0.15	S_5	1.9	S_{11}	3.05
W_5	22.53	S_0	4.81	S_6	1.58	S_{12}	3.2
W_6	1.66	S_1	5.08	S_7	8.96	D	4.0

that the total impedance of the short-circuited line is a combination of the impedance of the transmission line and the impedance of the grounded via. The length of the via remains constant and is equal to the substrate thickness. However, changes in the diameter of the via lead to variations in its equivalent impedance, including both real (resistance) and imaginary (inductance) components. Increasing the diameter (cross-section) of the via results in a decrease in its resistance and an increase in its inductive effect, which subsequently affects the input impedance of the entire line. This results in changes to both the amplitude and phase of reflection and transmission coefficients. To achieve the desired phase response and return loss, we modeled this effect using the CST tool and adjusted the diameter accordingly.

The radius of the via is changed from 1 mm to 3 mm, and its effect on the performance of the 90° main line (ports 1 and 2) is shown in Fig. 5. The results show when the via size increases the phase shift also increases and for the radius of 2 mm, we get the desired phase. By changing this parameter, the amount of the desired phase shift can be tuned. Fig. 5(d) also shows the isolation between adjacent ports according to the changing of the via radius. In this figure, at high frequencies, isolation is

better for the radius of 3 mm, but due to the broad operational bandwidth, phase, and loss performance, the optimal value of 2 mm is selected.

The second investigated parameter is the curving of the edges of the short-end coupled section of the 45° main line. This is shown in Fig. 6. In Fig. 7, the effects of the sharp/curved edge on the return loss and phase shift of the 45° line (ports 5 and 6) are illustrated. As can be seen, curving this edge reduces the reflection of the waves toward the input port. However, the phase shift of this line is affected by the edge curvature, which must be tuned through the optimization process.

(a)   (b)

(c)   (d)
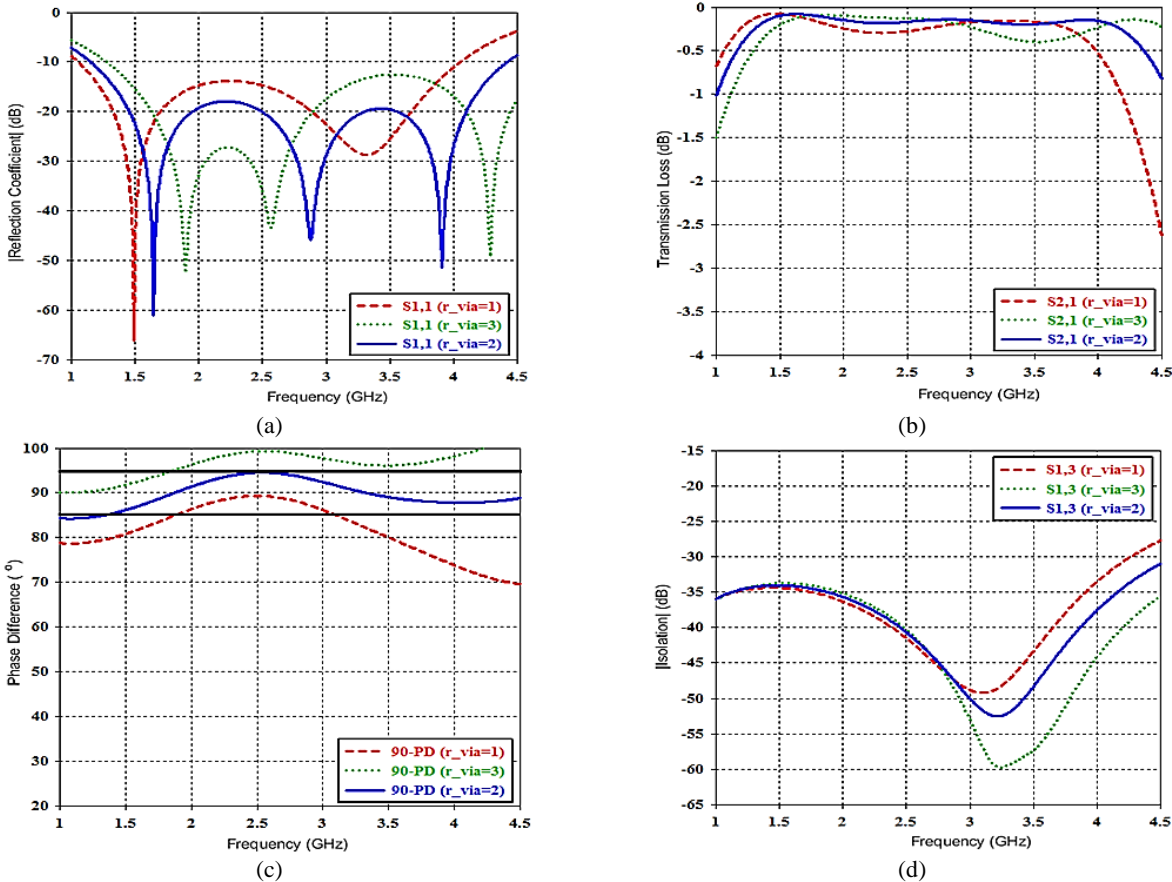
Fig. 5 The effect of the via size on the (a) return loss, (b) transmission loss, (c) phase shift of the 90° branch, and (d) isolation between adjacent ports of the 90° and reference lines.


(a)   (b)
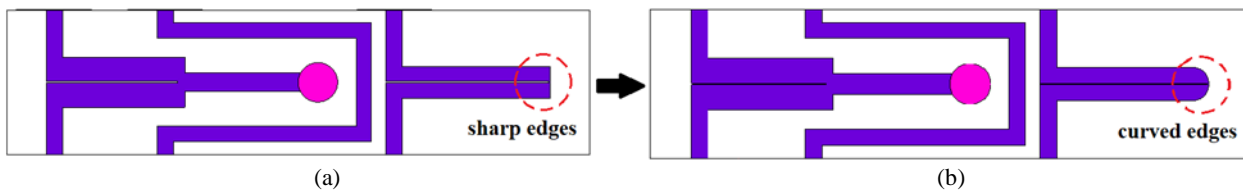
Fig. 6 Short-end coupled line of the 45° main line; (a) sharp edge, (b) curved edge.

3 Performance Evaluation of the Dual-Channel Phase Shifter

For verification, after simulation and obtaining the optimal parameters, a prototype of the phase shifter was fabricated, as shown in Fig. 8, and its results were measured. The measured S-parameters and phase response of the designed phase shifter are compared with the simulation in Figs. 9 -11. The return loss at the input ports, according to Fig. 9, is better than 16 dB over the frequency range of 1.26 GHz to 4 GHz (104% bandwidth). Since the structure is symmetric, only half of the S-parameters are reported. The maximum transmission losses at the output ports, including the loss introduced by SMA connectors, are less than 0.35 dB. According to Fig. 10, over the desired frequency range, a

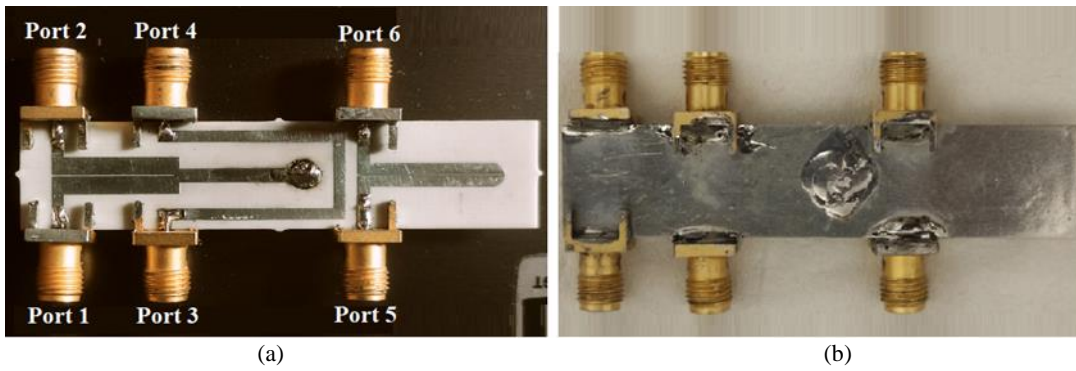phase difference of $90° ± 5°$ and $45° ± 5°$ is obtained   between the main lines and the common reference line.
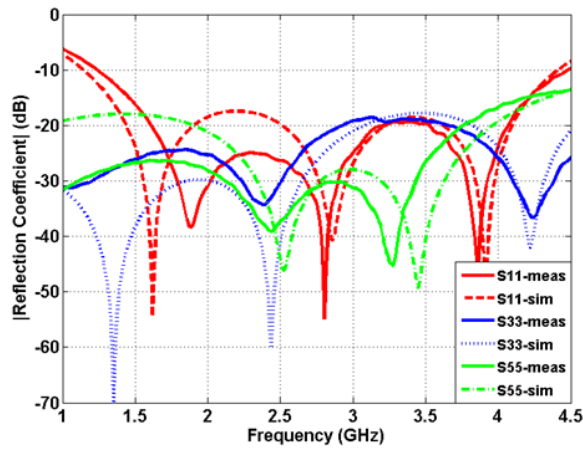

(a)
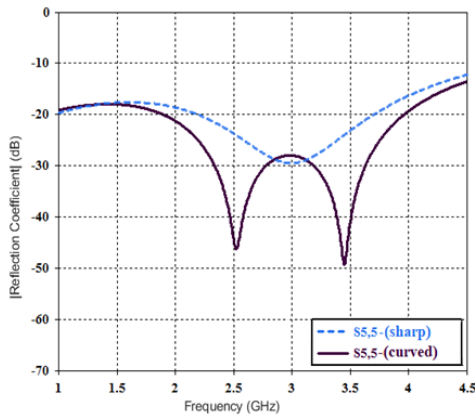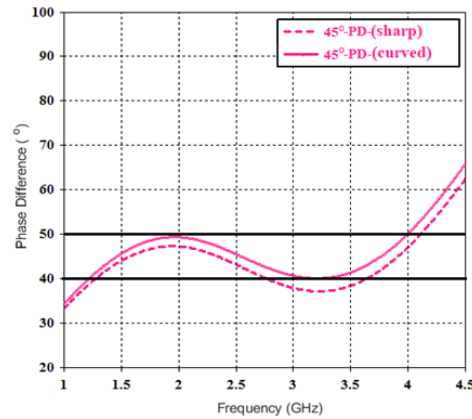
(b)

Fig. 7 The curving effect of coupled line edge of 45° line on (a) input return loss, (b) phase shift.
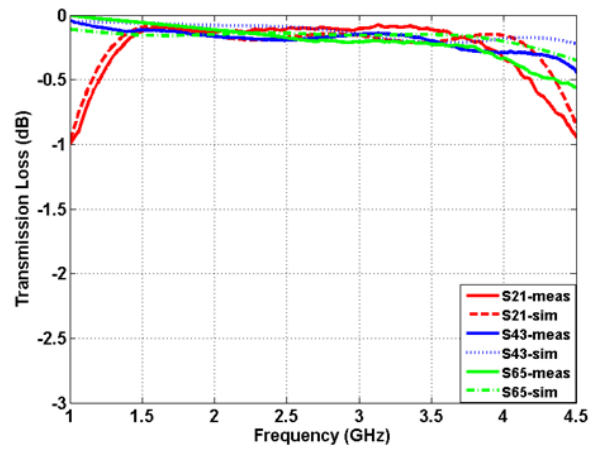

(a)

(b)

Fig. 8 Fabricated dual-channel phase shifter structure; (a) front, (b) back.


(a)

(b)

Fig. 9 (a) Comparison between the measured and simulated reflection coefficient and (b) transmission loss of the channels of the phase shifter.

In addition, Fig. 11 shows the isolation between adjacent ports; it is better than 32 dB between ports 1 and 3 and better than 20 dB between ports 3 and 5. Thus, the high isolation between adjacent ports does not degrade the performance of the phase shifter. There is a good agreement between the simulated and measured results. A slight discrepancy between them is mainly caused by

the fabrication errors in narrow coupling gaps and the loss introduced by SMA connectors, which are not included in the simulation.
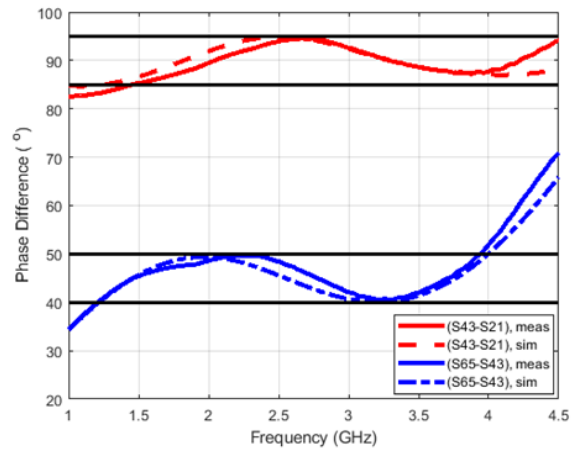
Table 2 compares the performance of the proposed phase shifter with the previously published works. The comparison shows the proposed dual-channel phase shifter has a compact size and achieves a maximum 5°

phase deviation over a wide bandwidth with the lowest
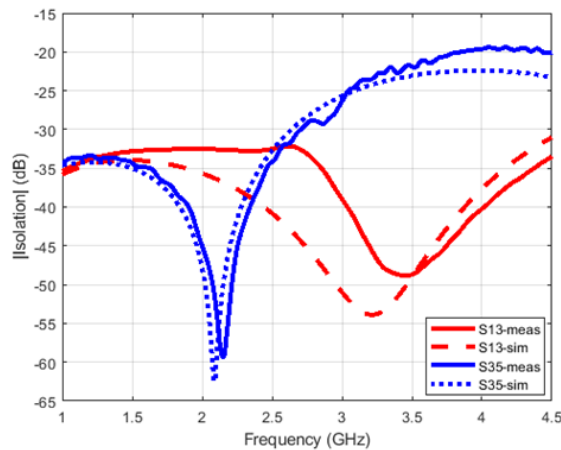
transmission loss of less than 0.35 dB.

(a)
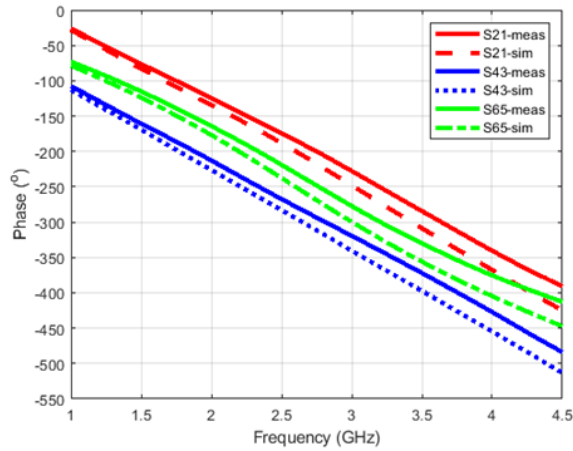
(b)

Fig. 10 (a) Phase at the output ports of the dual-channel phase shifter, (b) required phase shift: phase difference between the main lines and the reference line.

Table 2 Comparison of the proposed phase shifter with previous works.

Reference	Phase shift (°)	Number of layers	Size (λ_g^2)	Bandwidth (%)	Return loss (dB)	Transmission loss (dB)
[13]	90 ± 3.9	1	0.05×0.5	118	10	0.5
[20]	90 ± 6.7	1	0.06×0.51	81.9	10	0.53
[21]	90 ± 5	1	0.29×0.77	102.7	14.2	0.7
[22]	45 ± 2.3 ------- 90 ± 4.7	1	0.27×0.64 ------------- 0.35×0.78	82	15	0.64 ------------- 0.78
[23]	45 ± 2.1 ------- 90 ± 3.7	1	0.06×1.8	51	14.7	1 ------------- 1.1
This work	90 ± 5 ------- 45 ± 5	1	0.22×0.61 ------------- 0.22×0.37	104	>16	<0.35 ------------- <0.3

Fig. 11 Isolation between adjacent ports of the phase shifter.

4 Conclusion

In this paper, a wideband and low-loss dual-channel differential phase shifter is developed based on coupled microstrip lines. It has a maximum phase deviation of ±5° and a transmission loss of less than 0.35 dB over the broad bandwidth of 1.26 GHz – 4 GHz (104% bandwidth). Simple structure, low manufacturing cost, wide bandwidth, low transmission loss, and low phase error are some of the advantages of this phase shifter. The selected operational bandwidth in the design of this phase shifter includes important frequency bands such as GPS, DCS, PCS, WiBro, Bluetooth, WiMax, and WLAN. This phase shifter can be used in wireless networks and feeding networks of the array antennas.

References

[1] V.K. Varadan, K.J. Vinoy, and K.A. Jose, RF *MEMS and Their Applications*, New York: John

Wiley & Sons, 2002.

[2] A.M. Abbosh, "Ultra-wideband phase shifters," *IEEE Trans. Microw. Theory Tech*., vol. 55, no. 9, pp. 1935-1941, 2007.

[3] B.M. Schiffman, "A new class of broad-band microwave 90-degree phase shifters," *IRE Trans. Microw. Theory Tech.*, vol. 6, no. 2, pp. 232-237, 1958.

[4] J.P. Shelton and J.A. Mosko, "Synthesis and design of wide-band equal-ripple TEM directional couplers and fixed phase shifters," *IEEE Trans. Microw. Theory Tech.*, vol. 14, no. 10, pp. 462-473, 1966.

[5] J.L.R. Quirarte and J.P. Starski, "Novel Schiffman phase shifters," *IEEE Trans. Microw. Theory Tech.*, vol. 41, no. 1, pp. 9-14, 1993.

[6] Y.X. Guo, Z.Y. Zhang, and L.C. Ong, "Improved wide-band Schiffman phase shifter," *IEEE Trans. Microw. Theory Tech.*, vol. 54, no. 3, pp. 1196-1200, 2006.

[7] M. Sorn, R. Lech, and J. Mazur, "Simulation and experiment of a compact wideband 90° differential phase shifter," *IEEE Trans. Microw. Theory Tech.*, vol. 60, no. 3, pp. 494-501, 2012.

[8] L. Guo and A. Abbosh, "Phase shifters with wide range of phase and ultra-wideband performance using stub-loaded coupled structure," *IEEE Microw. Wirel. Compon. Lett.*, vol. 24, no. 3, pp. 167-169 2014.

[9] B. Elamaran, I. Chio, L. Chen, and J. Chiao, "A beam-steerer using reconfigurable PBG ground plane," *IEEE MTT-S Int. Microw. Symp.*, Boston, MA, USA, 2000.

[10] M.K. Mandal, A. Singh, and A. Bankar, "Low loss and high fabrication tolerant phase shifters using signal interference technique," *IET Microw. Ant. Propag.*, vol. 13, no. 11, pp. 1820-1825, 2019.

[11] D. Wang, E. Polat, H. Tesmer, R. Jakoby, and H. Maune, "Highly miniaturized continuously tunable phase shifter based on liquid crystal and defected ground structures," *IEEE Microw. Wirel. Compon. Lett.*, vol. 32, no. 6, pp. 519-522, 2022.

[12] S. Marini, J. Zbitou, R. Mandry, A. Errkik, A. Tajmouati, and M. Latrach, "Design of 45 degree microstrip phase shifter for beam forming network application using parallel coupled lines," *Int. Conf. Wirel. Tech., Embedded and Intelligent Systems (WITS)*, Fez, Morocco, 2017.

[13] Q. Liu, H. Liu, and Y. Liu, "Compact ultra-wideband 90° phase shifter using short-circuited stub and weak coupled line," *Electronics Lett*., vol. 50, no. 20, pp. 1454-1456, 2014.

[14] Y. Takeda, W. Withayachumnankul, and Y. Monnai, "Study of microstrip-based Terahertz phase shifter using liquid crystal," *44th Int. Conf. Infrared, Millimeter and Terahertz Waves (IRMMW-THz)*, Paris, France, 2019.

[15] B.T. Malik, V. Doychinov, and I.D. Robertson, "Compact broadband electronically controllable SIW phase shifter for 5G phased array antennas," *12th Euro. Conf. Ant. and Propag. (EuCAP)*, London, UK, 2018.

[16] H. Peng, Y. Wu, Y. Zuo, J. Dong, S.O. Tatu, Y. Liu, and T. Yang, "Synthesis design of equal-length phase shifter based on substrate integrated waveguide and microstrip line," *Int. J. RF Microw. Comput. Aided Eng.*, vol. 31, no. 3, pp. 1-8, 2021.

[17] T.N. Ross, G. Cormier, K. Hettak, and J.S. Wight, "High-power X-band GaN switched-filter phase shifter," *IEEE MTT-S Int. Microw. Symp. (IMS)*, Tampa, FL, USA, 2014.

[18] V. Puyal, D. Dubuc, K. Grenier, C. Bordas, O. Vendier, and J.L. Kazaux, "Design of robust RF-MEMS phase shifter in Ka-band," *Romanian J. Info. Sci. and Techn.*, vol. 11, no. 2, pp. 153-165, 2008.

[19] Y.P. Lyu, L. Zhu, and C.H. Cheng, "Synthesis design of filtering wide-band differential phase shifters on multimode resonators with controllable same insertion loss bandwidth," *IET Microw. Ant. Propag*., vol. 12, no. 3, pp. 367-374, 2018.

[20] Y. Wu, S. Zhou, X. Shen, and Y. Liu, "A compact and miniaturized broadband phase shifter using coupled-lines," *ACES J.*, vol. 31, no. 7, pp. 806-811, 2016.

[21] Y.P. Lyu, L. Zhu, and C.H. Cheng, "Single-layer broadband phase shifter using multimode resonator and shunt λ/4 stubs," *IEEE Trans. Compon., Packaging and Manufacturing Tech*., vol. 7, no. 7, pp. 1119-1125, 2017.

[22] W. Zhang, K. Xu, J. Shi, and Z. Shen, "A compact single-layer balanced phase shifter with wide bandwidth and uniform reference line," *IEEE Access*, vol. 8, pp. 41530-41536, 2020.

[23] Y. Nie, W. Zhang, and J. Shi, "A compact balanced phase shifter with wideband common-mode suppression," *IEEE Access*, vol. 7, pp. 153810-153818, 2019.

Robab Kazemi (Member, IEEE) received the B.S. degree in electrical engineering from Amir Kabir University of Technology (Tehran Polytechnic), Tehran, Iran, in 2004, and the M.S. and Ph.D. degrees from K. N. Toosi University of Technology, Tehran, in 2007 and 2012, respectively. From 2010 to 2011, she was a Visiting Research Scholar with the Department of Electrical Engineering and

Computer Science, the University of Tennessee, Knoxville, TN, USA, where she was a Visiting Assistant Professor in 2013 and 2016. She is currently an Associate Professor of electrical engineering at the University of Tabriz, Tabriz, Iran.

Her research interests include the design of passive microwave circuits, UWB antennas, antennas for medical applications, and electromagnetics.

Zohreh Assadollahzadeh Zia received the B.S. degree in Physics from the Islamic Azad University of Tabriz, Tabriz, Iran, in 2008 and the M.S. degree in electrical engineering from the University of Tabriz, Tabriz, Iran, in 2022, where she is currently pursuing a Ph.D. degree in electrical engineering.

Her research interests include UWB components, microstrip antennas, and microwave components design.

Reza Masoumi received the B.S.E.E. degree in 2014 from the University of Tehran, Tehran, Iran, the M.S.E.E degree in 2017 from Tarbiat Modares University, Tehran, Iran, and the Ph.D. degree in electrical engineering from the University of Tabriz, Tabriz, Iran, in 2023.

His research interests include electromagnetic invisibility and cloaking, UWB systems, beamforming, and 5G antennas.